Chapter 2
Polyarylether Hosts

2.1 Background

Since phosphorescent emitters generally show relatively long excited-state lifetimes and concentration quenching effect, they are usually doped in suitable hosts to achieve high efficiency [1–3]. So the selection of host materials is critical for fabricating efficient PhOLEDs. Basically, there are several requirements for host materials: (1) E_Ts higher than those of the dopants to prevent TEBT from dopants to hosts (for blue PhOLEDs, $E_T > 2.7$ eV is desirable) [4]; (2) excellent charge injection/transporting capability to achieve considerable charge flow in the emissive layer [5–7]; (3) high thermal and morphological stability to improve operation stability of devices. However, there is generally a dilemma between high E_T and high charge injection/transporting capability for polymer hosts. Polymer with high E_T always possesses high energy bandgap and thus high LUMO level or low HOMO level or both, leading to large charge injection barriers. To solve the problem, great efforts have been paid to developing new polymer host systems, and considerable progress has been achieved for polymer hosts used in green and red PhPLEDs [8–11]. However, polymer hosts suitable for blue PhPLEDs are extremely scarce.

Basically, the ever reported polymer hosts can be classified into two kinds: conjugated ones and nonconjugated ones. Conjugated polymers such as polycarbazoles (PCzs) and polyfluorenes (PFs) usually show low E_Ts (2.4–2.6 eV for PCzs [8] and $\sim$2.2 eV for PFs [9]) because of their large conjugation extent, so they can only host green and red phosphors. To fabricate blue PhPLEDs, the nonconjugated PVK host is most used. However, PVK is a unipolar conductor that transports holes only, so it must be blended with a large amount of electron transporting materials to achieve charge balance [12]. This physical blend system suffers from poor long-term device stability because of phase separation. Therefore, development of efficient novel polymeric hosts for blue PhPLEDs is challenging, but of great significance at present.

S. Shao, *Electrophosphorescent Polymers Based on Polyarylether Hosts*,
Springer Theses, DOI 10.1007/978-3-662-44376-7_2

2.2 Molecular Designs

In this thesis, we report the invention of a series of partially conjugated polyarylether hosts which possess both high E_Ts and bipolarity (Fig. 2.1) [13]. The motivation that we select the polyarylether scaffold is based on the following considerations: (1) the π-conjugation of the polyarylether backbone are interrupted because of the saturated oxygen atom, which will lead to high E_Ts; (2) polyarylethers take advantage of good thermal and morphological stability, which is beneficial for the reliability of the devices; (3) the synthesis of polyarylethers involves a nucleophilic aromatic substitution polycondensation without any residual catalyst contamination which is always a big problem in transition-metal-catalyzed conjugated light-emitting polymers [14]. Based on this polyarylether scaffold, triphenylphosphine oxide and carbazole/triphenylamine units are introduced into the main chain and side chain as electron and hole transport units, respectively, to endow the polymers with bipolar characteristic (PCzPO and PDPAPO, Fig. 2.2). In addition, to investigate the electronic structures of these polyarylethers in detail, their conjugated counterpart (PCzP and PDPAPO) are also designed for comparison.

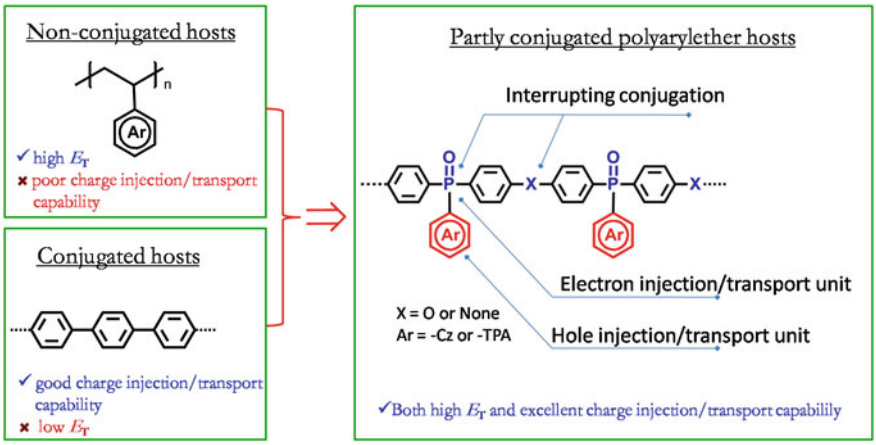

Fig. 2.1 Design strategy of the polyarylether hosts

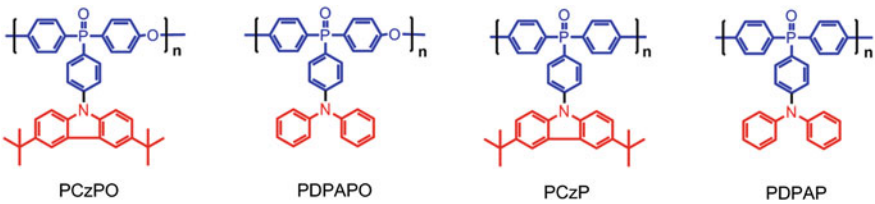

Fig. 2.2 Chemical structures of the polymer hosts

2.3 Results and Discussions

Synthesis and Characterization Scheme 2.1 shows the synthetic route of the polymer hosts. The bisarylphosphine oxide intermediates (**1**, **2**, **3**, **5**) were synthesized from diethylphosphite and corresponding arylmagnesium halides in good yields. The aryl halide intermediates (**6**, **7**, **8**) were produced by Cu-catalyzed *N*-arylization of carbazoles or diphenylamine with *para*-dibromobenzene or *para*-diiodobenzene. The triarylphosphine oxides (F-Cz-MON, F-DPA-MON, Br-Cz-MON, Br-DPA-MON, **9**, **10**) and the model compound (MC) were obtained by Pd-catalyzed coupling reaction between bisarylphosphine oxide and the corresponding aryl halides. In detail, the difluorinated monomers (F-Cz-MON and F-DPA-MON) and alkylsilyloxy precursors (**9**, **10**) can be readily obtained from aryl bromides with corresponding bisarylphosphine oxides. While for the dibrominated monomers (Br-Cz-MON and Br-DPA-MON), aryl iodides were superior in the coupling reaction. Deprotection of the alkylsilyloxy precursors (**9**, **10**) in acid afforded the dihydroxy monomer (HO-Cz-MON and HO-DPA-MON) in nearly quantitative yields. The polyarylether hosts PCzPO and PDPAPO were easily synthesized from the difluorinated monomers and the dihydroxy monomers under classical nucleophilic substitution condition; while the poly(arylene phosphine oxide) type polymer PCzP and PDPAP were synthesized from the dibrominated monomers according to the Yamamoto polymerization with Ni(0) catalyst. All the polymers exhibit good solubility in halogenated solvents such as dichloromethane, chloroform, and chlorobenzene. The number-average molecular weights of the polymers determined by gel permeation chromatography (GPC) with polystyrene as a standard ranges from 9,100 to 20,600 (Table 2.1).

The decomposition temperature (T_d) with 5 % weight-loss was determined by thermogravimetric analysis (TGA). As shown in Fig. 2.3 and Table 2.1, all the polymers show T_ds higher than 440 °C. In addition, the glass transition temperatures (T_g) of the polymers determined by differential scanning calorimetry (DSC) are higher than 200 °C. In special, compared with PCzPO and PDPAPO, PCzP and PDPAP show higher T_gs, indicating that the poly(arylene phosphine oxide) backbone is much more rigid than the oxygen-containing one. Nevertheless, it is noteworthy that T_gs of all the polymers are much higher than the conventional hosts such as polyfluorenes and poly carbazoles. The high T_gs as well as the high T_ds of these polymers endow them with excellent thermal and morphological stability, which is beneficial for the reliability of the light-emitting diodes.

Photophysical Properties The absorption and emission spectra of the polymers are shown in Fig. 2.4. All the polymers show strong absorption in the range of 300–350 nm attributed to the π-π* transition of the repeating units. The PL spectra of the polymers in toluene show similar profiles with peaks in the range of 390–410 nm. While the polymer films showed quite different PL spectra. The emission peaks of the conjugated counterparts (PCzP and PDPAP) were red-shifted by 40–50 nm relative

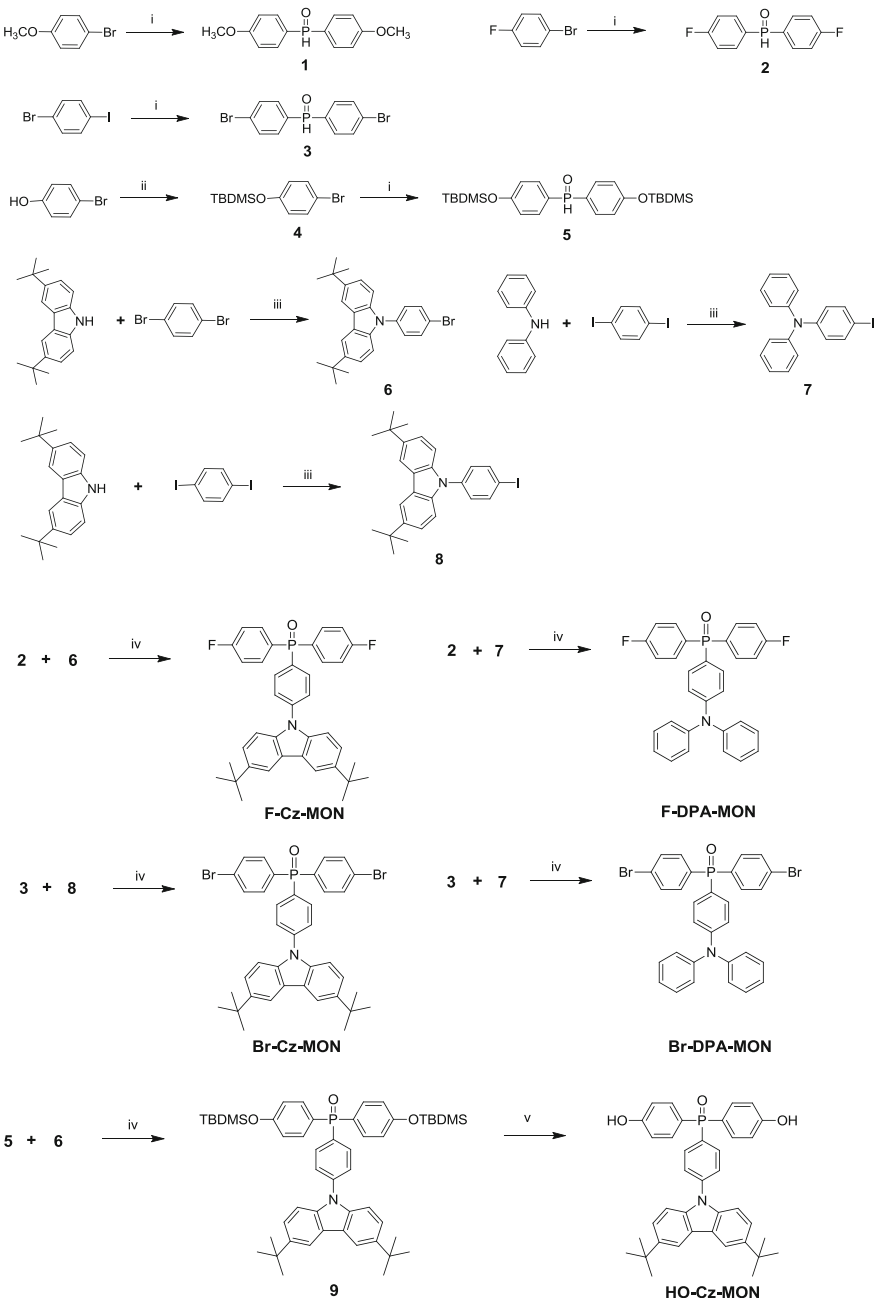

Scheme 2.1 Synthetic route of the polymer hosts. Reagents and conditions: (i) magnesium, THF and diethylphosphite; (ii) *tert*-butyldimethylsilyl chloride, triethylamine and CH_2Cl_2, 0 °C to room temperature; (iii) CuI, K_2CO_3, 1,2-dichlorobenzene and 18-crown-6; 190 °C; (iv) $Pd(PPh_3)_4$, *N*-methylmorpholine and toluene, 100 °C; (v) HCl, room temperature; (vi) BBr_3, CH_2Cl_2, −78 °C to room temperature; (vii) K_2CO_3, *N, N*-dimethylacetamide (DMAc), toluene 170 °C; (viii) Ni $(COD)_2$, COD, 2,2'-bipyridine (BPy), DMF, 80 °C

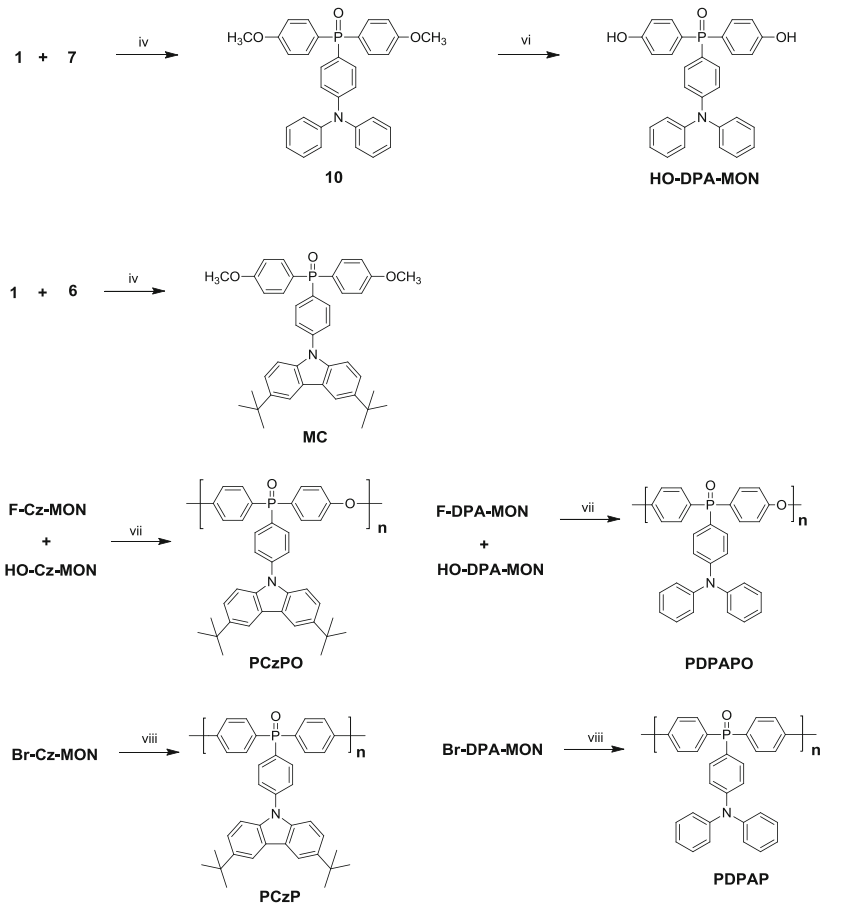

Scheme 2.1 (continued)

Table 2.1 Characterization data of the polymer hosts

Polymer	M_n^a	M_w^b	PDI[c]	T_d^d	T_g^e
PCzPO[f]	20,600	35,600	1.73	513	303
PDPAPO[g]	9,100	20,400	2.24	458	221
PCzP[f]	10,500	17,600	1.68	479	355
PDPAP[g]	10,100	24,100	2.39	448	303

[a] Number-average molecular weight
[b] Weight-average molecular weight
[c] Polydispersity index
[d] Decomposition temperature
[e] Glass transition temperature
[f] GPC performed with THF as the eluent
[g] With $CHCl_3$ as the eluent

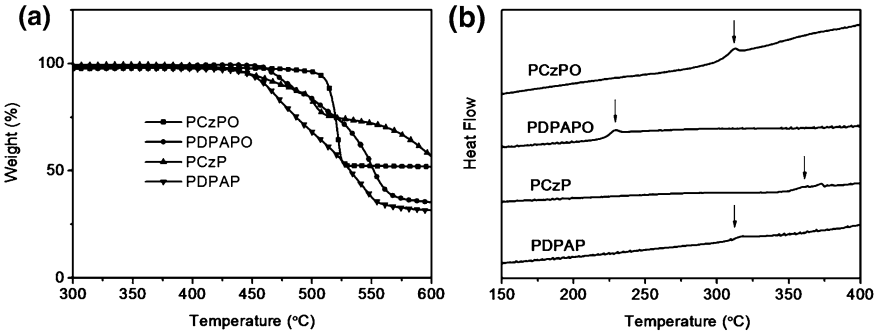

Fig. 2.3 TGA (**a**) and DSC curves (**b**) of the polymer hosts

to those of polyarylethers (PCzPO and PDPAPO). On the other hand, polymers with carbazole side chain (PCzPO and PCzP) showed blue-shifted peaks by 20–35 nm compared with the ones containing diphenylamine side chains (PDPAPO and PDPAP). These observations are consistent with the photo induced charge transfer process from the electron-rich sidechain to the electron-deficient main chain. Polymers with stronger electro-donating units (diphenylamine > carbazole, see below) and/or stronger electro-withdrawing segments (4,4′-bis(diphenylphosphine oxide) biphenyl > triphenylphosphine oxide) show emissions with much longer wavelength.

The phosphorescent spectra of these polymers were measured at 77 K (Fig. 2.5). E_Ts of the polymers were calculated according to the highest-energy triplet vibronic transition. As listed in Table 2.2, all the polymers show E_Ts higher than 2.70 eV, which have broken through the limitation of traditional conjugated polymer hosts. The high E_Ts ensure that these polymers are qualified to host blue phosphorescent emitters such as FIrpic (E_T = 2.62 eV). Considering that the E_Ts of PCzP and PDPAP are much higher than those of polyphenylenes (~2.20 eV), we propose that the introduction of P=O bond into the main chain reduces the conjugation length. As reported in previous studies, P=O bond inserted in aryl units plays the

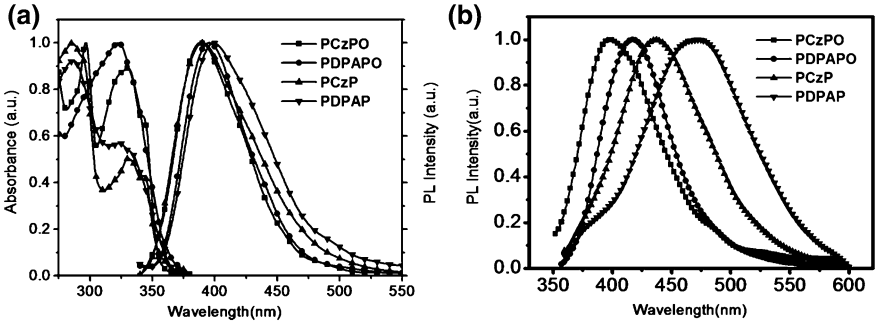

Fig. 2.4 **a** Absorption (in dichloromethane, 10^{-5} mol/L) and PL spectra (in toluene, 10^{-5} mol/L) of the polymer hosts. **b** PL spectra of the polymer films

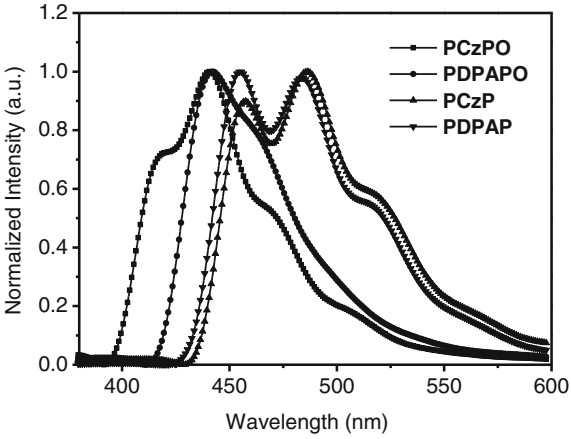

Fig. 2.5 Phosphorescent spectra of the polymer hosts at 77 K (in toluene, 10^{-3} mol/L)

Table 2.2 Photophysical and electrochemical properties of the polymer hosts

	$\lambda^{a}_{em,\ max}$ (nm)	$\lambda^{b}_{em,\ max}$ (nm)	$\lambda^{c}_{abs,\ onset}$ (nm)	E_T (eV)	HOMO (eV)	LUMO (eV)
PCzPO	389	397/417	354	2.96	−5.73	−2.26
PDPAPO	395	418	361	2.81	−5.52	−2.25
PCzP	391	437	354	2.73	−5.71	−2.76
PDPAP	399	466/475	362	2.71	−5.50	−2.78

[a] Emission peaks measured in toluene (10^{-5} mol/L)
[b] Emission peaks measured in film state
[c] Onset value of the absorption spectrum

role of an 'isolated site' so the electrons cannot be delocalized along the adjacent aryl rings [15]. In addition, we note that, compared with PCzP and PDPAP, E_Ts of PCzPO and PDPAPO are elevated by 0.10–0.23 eV. This result indicates that the incorporation of the saturated oxygen atom further interrupts the conjugation of the main chain. Consequently, with the synergistic effect of the oxygen atom and the P=O bond, PCzPO shows the highest E_T of 2.96 eV, which has greatly surpassed most reported polymer hosts in terms of triplet energy (Fig. 2.6).

Electrochemical properties Electrochemical properties of the polymers were investigated by the cyclic voltammetry (CV) (see Fig. 2.7a). The highest occupied molecular orbital (HOMO) and lowest unoccupied molecular orbital (LUMO) energy levels of the polymers are calculated according to their onsets of oxidation and reduction potentials, respectively. As listed in Table 2.2, the HOMO levels of PCzPO and PCzP are −5.73 and −5.71 eV, respectively; while those of PDPAPO and PDPAP were −5.52 and −5.50 eV, respectively. These values are very close to those of their side chain units (carbazole/triphenylamine units). The higher HOMO levels of PDPAPO and PDPAP than those of PCzPO and PCzP are resulted from the stronger electron-donating ability of triphenylamine compared with carbazole

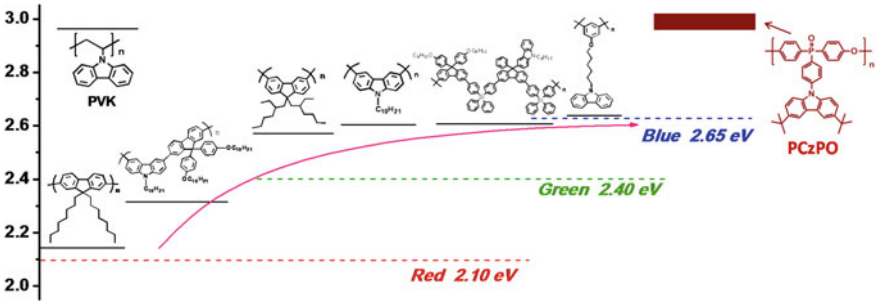

Fig. 2.6 Comparison of E_Ts of PCzPO and traditional polymer hosts

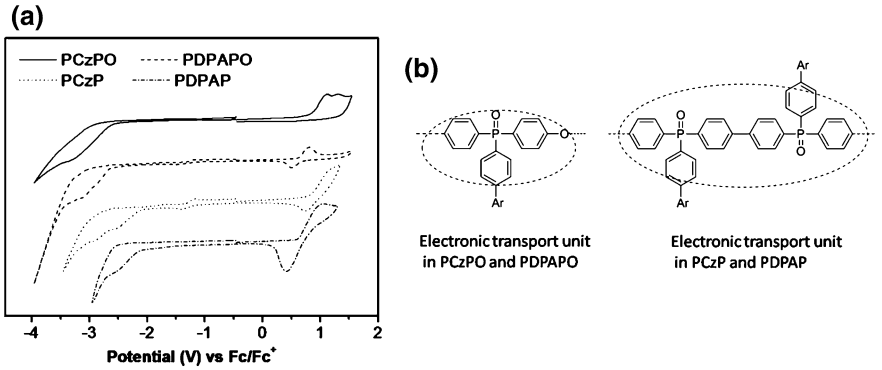

Fig. 2.7 CV curves of the polymer hosts (**a**) and electronic transporting units in the polymer hosts (**b**)

units. The LUMO levels of PCzP and PDPAP calculated from the reduction onsets are at −2.76 and −2.78 eV, respectively, which are about 0.5 eV lower than those of PCzPO and PDPAPO (∼−2.25 eV). This observation is reasonable considering that the LUMO energy level is determined by the triarylphosphine oxide segments, therefore the larger conjugation extent caused by the biphenyl units in PCzP and PDPAP mainchian results in lower LUMO level (Fig. 2.7b).

It is worthy to note that, the energy levels of our polymers match better with the common carrier transporting materials and electrodes than those of the widely used host PVK which shows a low HOMO level of −5.90 eV and a high LUMO level of −2.10 eV. The lowered energy barriers between the emissive layer and the adjacent layers are beneficial for the charge injection in the EL process and are expected to enhance the power efficiency of the devices.

Electroluminescent properties In view of the high E_Ts of these polymers, we explore their potential as host materials for blue phosphors. PhPLEDs with typical device architectures of glass/ITO/PEDOT:PSS (40 nm)/polymer hosts: 5 wt% FIrpic (40 nm)/TPCz (50 nm)/LiF (1 nm)/Al (200 nm) were fabricated (Fig. 2.8). Here, TPCz stands for 3,6-bis(diphenylphosphoryl)-9-(4-(diphenylphosphoryl)

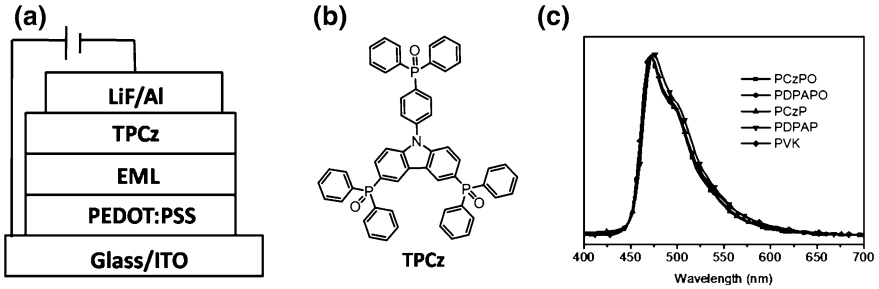

Fig. 2.8 Device configuration (**a**), chemical structure of TPCz (**b**) and EL spectra of the blue devices (**c**)

phenyl)- 9H-carbazole which acts as a hole/exciton blocking material [16]. All the devices show blue EL with a maximum emission peak at 472 nm typical for the emission of FIrpic with no trace of host emission, indicating an efficient energy transfer from the hosts to FIrpic.

The current density (J)–voltage (V)–brightness (B) and luminous efficiency (η_l)–current density (J)–power efficiency (η_p) curves are given in Fig. 2.9. The device performance is summarized in Table 2.3. The turn-on voltages of the devices are 5.3 ~ 5.8 V. Devices based on PDPAPO and PCzPO show very promising efficiency with the maximum η_l reaching 23.3 and 20.4 cd A^{-1}, respectively, which correspond to external quantum efficiency (EQE) of 10.8 and 10.0 %, respectively. We believe that both the high E_Ts of PCzPO and PDPAPO and the good carrier injection/transport capability account for the high η_l. In contrast, devices based on PCzP and PDPAP show relatively low η_l of 12.4 and 5.5 cd A^{-1}, respectively. The higher efficiency of PCzPO and PDPAPO than PCzP and PDPAP is reasonable considering that (1) E_Ts of PCzPO and PDPAPO are higher than those of PCzP and PDPAP, which leads to more effective confinement of the triplet excitons on the phosphors; (2) the electron flow in PCzP and PDPAP are comparable with or slightly higher than the hole flow (shown in Fig. 2.10), so considerable electric leakage that leads to the loss of carriers may occur in the PEDOT/(PCzP or PDPAP) interface, which is not prone to occur in PCzPO or PDPAPO-based devices.

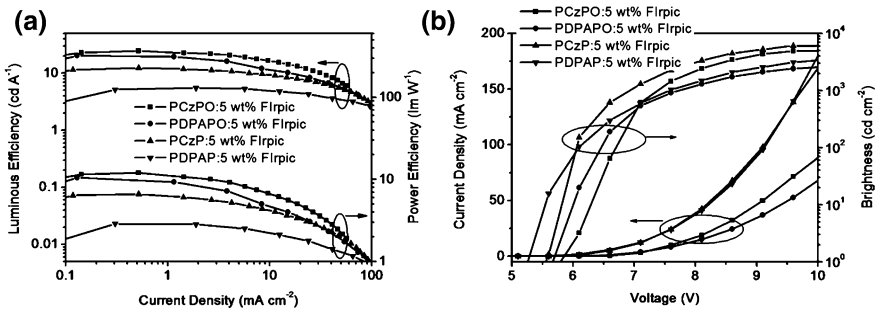

Fig. 2.9 η_l–J–η_p (**a**) and J–V–B (**b**) curves of the blue devices

Table 2.3 Device performance of the double-layer blue devices

Polymer	V_{on}^{a} (V)	$\eta_{l,\ max}^{b}$ (cd A^{-1})	$\eta_{p,\ max}^{c}$ (lm W^{-1})	EQE[d] (%)	L_{max}^{e} (cd m^{-2})	CIE[f] (x, y)
PCzPO	5.8	23.3	10.6	10.8	4,860	0.16, 0.30
PDPAPO	5.6	20.4	10.5	10.0	2,603	0.16, 0.31
PCzP	5.5	12.4	6.6	6.1	6,040	0.16, 0.31
PDPAP	5.3	5.5	2.9	2.7	3,484	0.17, 0.34

[a] Turn-on voltage
[b] Maximum luminous efficiency
[c] Maximum power efficiency
[d] Maximum external quantum efficiency
[e] Maximum luminance
[f] CIE coordinates

Since all the polymers contain triarylphosphine oxide units as the electron-transport units and carbazole/triphenylamine units as the hole-transport units, we propose that such polymers should exhibit bipolar characteristics. To confirm this speculation, single-carrier devices were prepared. The hole-only devices contain the following structure: ITO/PEDOT:PSS (50 nm)/Polymer (100 nm)/Au(100 nm), while the electron-only devices contain layers of Al (50 nm)/Polymer (100 nm)/Ca (10 nm)/Al (100 nm). For comparison, control devices using PVK as the active layer were also fabricated.

As Fig. 2.10 shows, PVK shows significantly larger hole flow than electron flow at applied voltage of 7 V ~ 20 V. Whereas in our hosts, the electron flow is significantly enhanced and becomes comparable with the hole flow. Besides, the following points can also be concluded from Fig. 2.10: first, the electron flow of PCzP and PDPAP is larger than that of PCzPO and PDPAPO, which is consistent with the much smaller electron-injection barriers for PCzP and PDPAP induced by their lower LUMO levels; secondly, the electron current of PCzP and PDPAP are in the same order of magnitude as their hole current, which is the foundation for the fabrication of efficient single-layer blue phosphorescent devices as discussed below.

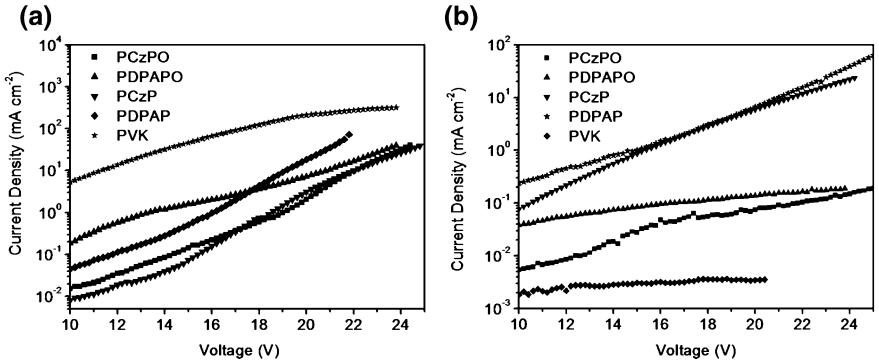

Fig. 2.10 *J–V* curves of the hole- (**a**) and electron-only (**b**) devices

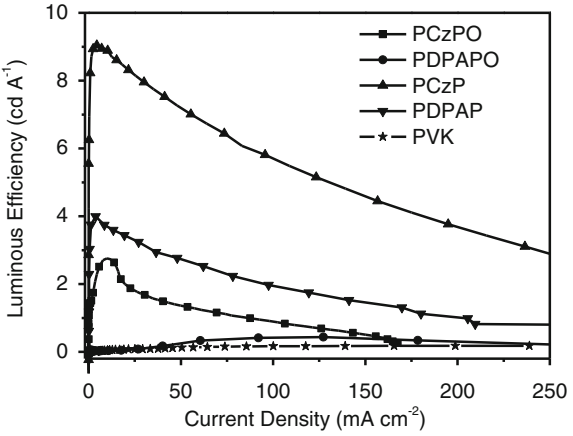

Fig. 2.11 η_l–J curves of the single-layer blue devices

The excellent bipolar characteristic of our polymers is also supported by the performance of the single-layer blue devices with the configuration of ITO/PEDOT: PSS (50 nm)/Polymer: 5 wt% FIrpic/Ca (10 nm)/Al(100 nm).

As shown in Fig. 2.11, all the polymers show higher η_l than PVK under the same current density, implying the much more balanced carriers in the polymers than in PVK. On the other hand, η_l of PCzP and PDPAP is much higher than those of PCzPO and PDPAPO, suggesting that in PCzP and PDPAP, carriers are much more balanced than those in PCzPO and PDPAPO. This observation is in agreement with the single-carrier device results. Among them, devices based on PCzP exhibit the highest luminous efficiency, which reaches 9.0 cd A^{-1}, indicating that PCzP is the most promising host for the fabrication of high-efficiency single-layer devices.

In order to fully exploit the potential of PCzP as a host for single layer devices, we prepared single layer blue, green, and red devices based on PCzP. FIrpic, G1, R1 are selected as the blue, green and red dopant, respectively (see Fig. 2.12). The optimized device structure is glass/ITO/PEDOT: PSS (40 nm)/PCzP: FIrpic or G1 or R1 (100 nm)/CsF (1 nm)/Al (200 nm). Wherein, the optimized doping content of FIrpic, G1 and R1 are 7.5, 30 and 2.5 wt%, respectively. EL spectra of the devices are shown in Fig. 2.13. The emission peaks are located at 476, 540 and 628 nm, corresponding to CIE coordinates of (0.17, 0.35), (0.41, 0.57), and (0.64, 0.35), respectively.

Fig. 2.12 Device structure of the single layer devices as well as the chemical structures of PCzP and the dopants

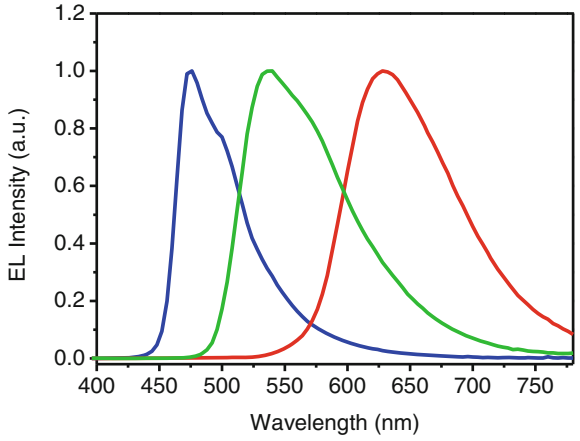

Fig. 2.13 EL spectra of the blue, green, and red devices based on PCzP

As Fig. 2.14 shows, V_{on} of the blue device is 5.7 V, while the maximum η_l, η_p and EQE are 9.8 cd A^{-1}, 4.0 lm W^{-1}, and 4.4 %, respectively. These values, to the best of our knowledge, are the highest ones reported for single-layer blue devices until now. Furthermore, the PCzP-based device shows a very small efficiency roll-off. At a brightness level of 1,000 and 5,000 cd m^{-2}, the luminous efficiency still retain as high as 9.6 and 8.1 cd A^{-1}, respectively. The small efficiency roll-off gives another evidence that the hole and electron flow in the emissive layer is balanced.

The maximum η_l, η_p and EQE of the green device reach 32.3 cd A^{-1}, 21.5 lm W^{-1} and 9.8 %, respectively (Table 2.4). Again the device shows a very small efficiency roll-off with the luminous efficiency retain as high as 31.9 and 27.5 cd A^{-1} at a brightness level of 1,000 and 5,000 cd m^{-2}, respectively. We note that these efficiencies are even comparable with those obtained with many double-layer devices [8–10, 17], indicating that the bipolar PCzP is competent for both the hole and electron injection/transport. Red device with 2.5 wt% R1 as the dopant shows maximum η_l, η_p and EQE of 4.9 cd A^{-1}, 1.4 lm W^{-1}, and 4.9 %, respectively. At a brightness level of 1,000 and 5,000 cd m^{-2}, the luminous efficiency

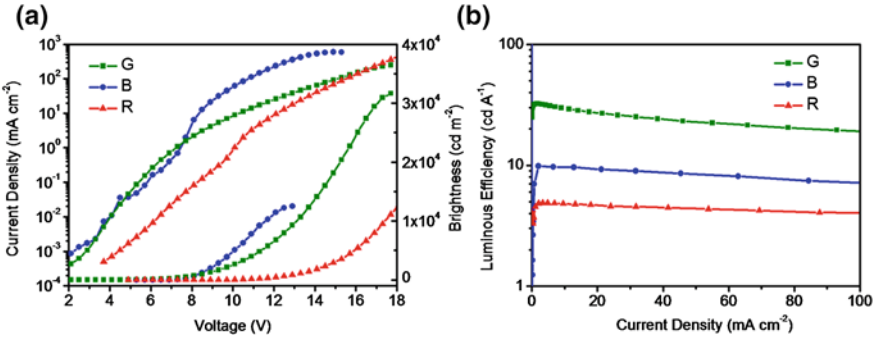

Fig. 2.14 *J–V–B* (**a**) and η_l–*J* curves (**b**) of the blue, green and red single layer devices

Table 2.4 Device performance of the blue, green, and red single-layer devices

Device	V_{on} (V)	$\eta_{l,\ max}$ (cd A^{-1})	$\eta_{p,\ max}$ (lm W^{-1})	EQE (%)	L_{max} (cd m^{-2})	CIE (x, y)
7.5 wt% Firpic: PCzPO	5.7	9.8	4.0	4.4	12,500	0.17, 0.35
30 wt% G1: PCzPO	3.7	32.3	21.5	9.8	31,675	0.41, 0.57
2.5 wt% R1: PCzPO	6.5	4.9	1.4	4.9	13,686	0.64, 0.35

retains as high as 4.6 and 3.9 cd A^{-1}, respectively. These values are also among the highest ones ever reported for red PhPLEDs. These results are encouraging considering that PCzP is so far the only one which can be used as the host material for all the blue, green, and red single layer devices. We believe that excellent performance based on PCzP comes from its high triplet energy levels and its good bipolar characteristic.

In conclusion, we have designed and synthesized a series of bipolar, high triplet energy polyarylether hosts containing triphenylphosphine oxide units as electron-transport main chain and carbazole/triphenylamine units as hole-transport side chain. The polymers show E_Ts as high as 2.96 eV because of the interrupted conjugation induced by the synergistic effect of P = O bond and saturated oxygen atom in the main chain. This achievement has broken through the limitation of traditional conjugated polymer hosts in terms of triplet energy. Blue PhPLEDs based on PCzPO with a double layer configuration exhibits a very promising luminous efficiency of 23.3 cd A^{-1}, which is among the highest ones ever reported for blue PhPLEDs.

Besides high E_Ts, the polymers show excellent bipolar characteristic compared with the traditional PVK host. Because of the simultaneous incorporation of hole and electron injection/transport units, the polymers show much lower energy barriers for the carrier injection, and much more balanced carrier flow compared with PVK. As a result, all the polymers show much lower driving voltage and higher efficiency for the simple single-layer blue device. Especially, PCzP with the most balanced carrier flow shows maximum luminous efficiency of 9.8, 32.3, and 4.8 cd A^{-1} for blue, green, and red single-layer devices, respectively. This result is encouraging considering that PCzP is so far the only one which can be used as the host material for all blue, green, and red single-layer devices.

The significance of this work is that it provides the only known bipolar, high triplet energy polymer host system for blue PhPLEDs. We believe that our study will push forward the development of the PhPLEDs in such a way that the molecular design strategy in this work enlightens researchers to develop rich and varied polymer hosts for PhPLEDs, especially for blue ones. In addition, the importance of these polymers is further emphasized by the fact that they afford a unique platform for the construction of electrophosphorescent polymers which have been recognized as a very promising kind of materials for fabricating efficient, stable, and low-cost PhPLEDs.

2.4 Experimental Section

General Information All chemicals and reagents were used as received from commercial sources without further purification. Solvents for chemical synthesis were purified according to the standard procedures. ^{1}H NMR spectra were recorded with a Bruker Avance 300 NMR spectrometer. Elemental analysis was performed using a Bio-Rad elemental analysis system. MALDI-TOF mass spectra were performed on an AXIMA CFR MS apparatus (COMPACT). TPCz and FIrpic were prepared in our lab.

Measurements and Characterization Molecular weight of the polymers were determined by gel permeation chromatography (GPC) on a Waters 410 instrument with polystyrene as the standard and THF/$CHCl_3$ as the eluent. Thermal properties of the polymers were analyzed with a Perkin-Elmer-TGA 7 instrument under nitrogen at a heating rate of 10 °C/min. UV–visible (UV–vis) absorption and photoluminescent spectra were measured with a Perkin-Elmer Lambda 35 UV–vis spectrometer and a Perkin-Elmer LS 50B spectrofluorometer, respectively. Phosphorescent spectra at 77 K were measured in toluene. Cyclic Voltammetry experiments were performed on an EG&G 283 (Princeton Applied Research) potentiostat/galvanostat system. The samples were tested in acetonitrile using ferrocene as an internal reference and n-Bu_4NClO_4 as the supporting electrolyte. The HOMO energy levels were calculated according to the equation $E_{HOMO} = -e[E_{onset,\ ox} + 4.8\ V]$, in which $E_{onset,\ ox}$ was the onset of the oxidation potential. The LUMO energy levels were calculated according to the equation $E_{LUMO} = -e[E_{onset,\ red} + 4.8\ V]$, where $E_{onset,\ red}$ was the onset of the reduction potential.

PLED Fabrication and Measurements To fabricate PLEDs, a 40-nm-thick PEDOT:PSS film was first deposited on the pre-cleaned ITO-glass substrates (20Ω per square) and subsequently baked at 120 °C for 40 min. For single-layer blue PhPLEDs, FIrpic was doped into the hosts (PCzPO or PVK) and spin-coated onto PEDOT:PSS as the emissive layer (EML). The thickness of the EML was about 100 nm. Successively, a 10-nm-thick film of Ca (or 1 nm CsF), and a 200-nm-thick film of Al were thermally evaporated on top of the EML at a base pressure less than 10^{-6} Torr (1 Torr = 133.32 Pa) through a shadow mask with an array of 10 mm^2 openings. The double-layer device was fabricated by the same method except that a 50-nm-thick film of TPCz was evaporated before deposition of 1 nm LiF and 200 nm Al. Hole-only and electron-only devices were fabricated according to the similar procedure with the structure of glass/ITO/PEDOT:PSS (40 nm)/PCzPO (130 nm)/Au (60 nm) and glass/PEDOT:PSS (40 nm)/Al (100 nm)/PCzPO (130 nm)/Ca (10 nm)/Al (200 nm), respectively. The EL spectra and CIE coordinates were measured using a PR650 spectra colorimeter. The current–voltage and brightness–voltage curves of devices were measured using a Keithley 2400/2000 source meter and a calibrated silicon photodiode. All the measurements were carried out at room temperature under ambient conditions.

Synthesis **1**. Diethylphosphite (0.91 mL, 7.08 mmol) was added dropwise at 0 °C to a solution of 4-methoxyphenylmagnesium bromide in tetrahydrofuran which was

prepared from 4-bromoanisole (3 mL, 23.4 mmol) and magnesium (0.674 g, 28.1 mmol). The mixture was aged for 30 min at 0 °C, then stirred at ambient temperature for 16 h. After that it was cooled again to 0 °C, and 75 mL NH_4Cl aqueous was then added slowly. The mixture was extracted with diethyl ether and the organic phase was washed with brine, then it was dried over Na_2SO_4. After the solvent had been completely removed, the residue was purified by column chromatography on silica gel using petroleum ether/ethyl acetate = 1/1 as eluent to give the product in 75 % yield. ^{1}H NMR (300 MHz, $CDCl_3$, δ): 8.03 (d, J = 477.6 Hz, 1H), 7.61 (dd, J = 13.1, 8.5 Hz, 4H), 6.99 (dd, J = 8.6, 1.8 Hz, 4H), 3.85 (s, 6H).

2. This compound was prepared from 4-fluorophenylmagnesium bromide and diethylphosphite according to the procedure for the synthesis of **1**. Column chromatography on silica gel using petroleum ether/ethyl acetate = 1/1 as eluent gave the product as a white solid in 72 % yield. ^{1}HNMR (300 MHz, $CDCl_3$, δ): 8.09 (d, J = 467.7 Hz, 1H), 7.75–7.66 (m, 4H), 7.25–7.18 (m, 4H).

3. This compound was prepared from 4-bromophenylmagnesium iodide and diethylphosphite according to the procedure for the synthesis of **1**. Column chromatography on silica gel using petroleum ether/ethyl acetate = 1/1 as eluent gave the product as a white solid in 55 % yield. ^{1}H NMR (300 MHz, $CDCl_3$, δ) 8.02 (d, J = 487 Hz, 1H), 7.65 (dd, J = 8.3, 2.2 Hz, 4H), 7.53 (dd, J = 13.2, 8.3 Hz, 4H).

4. To a stirred solution of 4-bromophenol (12.24 g, 70.8 mmol) in 50 mL of dry CH_2Cl_2 at 0 °C was added triethylamine (12.30 mL, 84.9 mmol) and then a solution of tert-butyldimethylsilyl chloride (12.8 g, 84.9 mmol) in 75 mL dry CH_2Cl_2. After that, the reaction mixture was warmed to room temperature, stirred for 24 h, and washed with hydrochloric acid (1 mol/L), followed by washing with brine. The organic phase was dried over Na_2SO_4. The solution was concentrated and the crude product was purified by silica gel column, giving a colorless oil in 99 % yield. ^{1}HNMR (300 MHz, $CDCl_3$, δ): 7.33 (d, J = 8.8 Hz, 2H), 6.73 (d, J = 8.8 Hz, 2H), 0.99 (s, 18H), 0.20 (s, 12H).

5. This compound was prepared from 4-((*tert*-butyldimethylsilyl)oxyl) phenylmagnesium bromide and diethylphosphite according to the procedure for the synthesis of **1**. Column chromatography on silica gel using petroleum ether/ethyl acetate = 1/1 as eluent gave the product as a light yellow oil in 63 % yield. ^{1}HNMR (300 MHz, $CDCl_3$, δ): 8.01 (d, J = 487 Hz, 1H), 7.56 (dd, J = 13.2, 8.4 Hz, 4H), 6.93 (dd, J = 8.4, 2.0 Hz, 4H), 0.98 (s, 18H), 0.22 (s, 12H).

6. A mixture of *p*-dibromobenzene (6.41 g, 27.2 mmol), 3,6-di-tert-butyl-9H-carbazole (2.53 g, 9.1 mmol), CuI (0.17 g, 0.9 mmol), 18-crown-6 (0.09 g, 0.3 mmol), K_2CO_3 (2.50 g, 18.1 mmol) and *o*-dichlorobenzene (2 mL) was heated at 180 °C for 8 h under argon. After cooling to room temperature, the mixture was extracted with CH_2Cl_2, washed with ammonia and then water, and dried over Na_2SO_4. After the solvent had been completely removed, the residue was purified by column chromatography on silica gel using petroleum ether as eluent to give the title product in 80 % yield. ^{1}HNMR (300 MHz, $CDCl_3$, δ): 8.13 (d, J = 1.8 Hz, 2H),

7.70 (d, J = 8.7 Hz, 2H), 7.46 (dd, J = 8.7, 2.1 Hz, 2H) 7.43 (d, J = 8.7 Hz, 2H), 7.31 (d, J = 8.7 Hz, 2H), 1.46 (s, 18H).

7. This compound was prepared from diphenylamine and *p*-diiodobenzene according to the procedure for the synthesis of **6**. Column chromatography on silica gel using petroleum ether as eluent gave the product in 45 % yield. ^{1}HNMR (300 MHz, $CDCl_3$, δ) 7.49 (d, J = 8.5 Hz, 2H), 7.28–7.23 (m, 6H), 7.08–7.01 (m, 6H), 6.82 (d, J = 8.5 Hz, 2H).

8. This compound was prepared from 3,6-di-tert-butyl-9H-carbazole and *p*-diiodobenzene according to the procedure for the synthesis of **6**. Column chromatography on silica gel using petroleum ether as eluent gave the product in 66 % yield. ^{1}HNMR (300 MHz, $CDCl_3$, δ) 8.12 (d, J = 1.8 Hz, 2H), 7.90 (d, J = 8.6 Hz, 2H), 7.46 (dd, J = 8.7, 1.9 Hz, 2H), 7.32 (d, J = 8.7 Hz, 4H), 1.46 (s, 18H).

F-Cz-MON. **2** (0.24 g, 1.0 mmol), **6** (0.48 g, 1.1 mmol), *N*-methylmorpholine (0.15 g, 1.5 mmol) and tetrakis(triphenylphosphine)palladium(0) (0.23 g, 0.2 mmol) was added consecutively to 7 mL toluene under argon. The mixture was then heated at 105 °C for 8 h. After cooling to room temperature, the obtained suspension was directly applied to a silica gel column using petroleum ether/ethyl acetate = 2/1 as eluent to give the crude product. Crystallizing from a mixture of petroleum ether and CH_2Cl_2 gave the pure product as white crystal in a yield of 91 %. ^{1}H NMR (300 MHz, $CDCl_3$, δ): 8.13 (s, 2H), 7.87–7.72 (m, 8H), 7.47 (dd, J = 8.7, 1.7 Hz, 2H), 7.42 (d, J = 8.7 Hz, 2H), 7.23 (d, J = 8.5 Hz, 4H), 1.46 (s, 18H). ^{13}C NMR (75 MHz, $CDCl_3$, δ): 166.5, 163.9, 143.7, 142.1, 138.4, 134.5, 133.5, 129.1, 126.3, 123.8, 116.4, 116.1, 109.1, 34.7, 31.9. ^{31}P NMR ($CDCl_3$, 295 K, δ): 26.80. MALDI-TOF MS: calcd for $C_{38}H_{36}F_2NOP$: 591.25. found: 592.2 $[M + H]^+$. Anal. calcd for $C_{38}H_{36}F_2NOP$: C, 77.14; H, 6.13; N, 2.37. found: C, 77.02; H, 6.01; N, 2.29.

9. This compound was prepared from **5** and **6** according to the procedure for the synthesis of F-Cz-MON. Column chromatography on silica gel using petroleum ether/ethyl acetate = 2/1 as eluent gave the product in 82 % yield. ^{1}H NMR (300 MHz, $CDCl_3$, δ): 8.13 (d, J = 1.7 Hz, 2H), 7.85 (dd, J = 11.4, 8.4 Hz, 2H), 7.68 (dd, J = 8.4, 2.2 Hz, 2H), 7.61 (dd, J = 11.6, 8.6 Hz, 4H), 7.47 (dd, J = 8.6, 1.7 Hz, 2H), 7.42 (d, J = 8.6 Hz, 2H), 6.96 (dd, J = 8.6, 2.3 Hz, 4H), 1.46 (s, 18H), 0.99 (s, 18H), 0.24 (s, 12H).

HO-Cz-MON. **9** was dissolved in a mixture of tetrahydrofuran and hydrochloric acid (2 M) and then stirred at room temperature for 48 h. The mixture was extracted with ethyl acetate and the organic phase was washed with $NaHCO_3$ aqueous and brine and then dried over Na_2SO_4. After complete removal of the solvent, the crude product was purified by column chromatography on silica gel with dichloromethane/methanol = 20/1 as eluent to give the product in quantitative yield. ^{1}H NMR (300 MHz, DMSO-d_6, δ): 10.23 (s, 2H), 8.30 (d, J = 1.4 Hz, 2H), 7.80 (d, J = 7.2 Hz, 4H), 7.52–7.41 (m, 8H), 6.94 (dd, J = 8.6, 2.2 Hz, 4H), 1.41 (s, 18H). ^{13}C NMR (75 MHz, DMSO-d_6) δ: 160.6, 143.0, 140.2, 137.9, 133.6, 133.3, 125.6, 123.8, 123.2, 122.8, 121.7, 116.7, 115.6, 109.2, 34.5, 31.7. ^{31}P NMR (DMSO-d_6, 295 K, δ): 24.97. MALDI-TOF MS: calcd for $C_{38}H_{38}NO_3P$: 587.26. found: 588.3

$[M + H]^+$. Anal. calcd for $C_{38}H_{38}NO_3P$: C, 77.66; H, 6.52; N, 2.38. found: C, 77.50; H, 6.48; N, 2.31.

F-DPA-MON. This compound was prepared from **2** and **7** according to the procedure for the synthesis of F-Cz-MON. Column chromatography on silica gel using petroleum ether/ethyl acetate = 3/2 as eluent gave the product in 82 % yield. ^{1}H NMR (300 MHz, $CDCl_3$) δ 7.72–7.64 (m, 4H), 7.41–7.28 (m, 6H), 7.19–7.10 (m, 10H), 7.03–6.90 (m, 2H). ^{13}C NMR (75 MHz, $CDCl_3$) δ: 166.3, 163.8, 151.4, 146.4, 134.6, 134.5, 134.4, 133.1, 133.0, 129.6, 128.3, 125.9, 124.6, 122.9, 121.8, 120.0, 119.9, 116.0, 115.9, 115.8, 115.7. ^{31}P NMR ($CDCl_3$, 295 K, δ): 27.25. MALDI-TOF MS: calcd for $C_{30}H_{22}F_2NOP$: 481.1 found: 482.1 $[M + H]^+$. Anal. calcd for $C_{30}H_{22}F_2NOP$: C, 74.84; H, 4.61; N, 2.91. found: C, 74.64; H, 4.55; N, 2.83.

10. This compound was prepared from **1** and **7** according to the procedure for the synthesis of F-Cz-MON. Column chromatography on silica gel using petroleum ether/ethyl acetate = 1/1 as eluent gave the product in 90 % yield. The crude product was used directly in the following step.

HO-DPA-MON. **10** (1.80 g, 3.6 mmol) was dissolved in 20 mL dry dichloromethane. Then the solution was cooled to −78 °C and then BBr_3 (1.8 M in dichloromethane, 8 mL, 14.2 mmol) was added. After that, the reaction mixture was warmed to room temperature, stirred for 24 h, and poured into cold water. The mixture was then extracted with ethyl acetate and the organic layer was washed with $NaHCO_3$ aqueous and water. After drying, the organic layers was concentrated and applied to a silica gel column using CH_2Cl_2/CH_3OH = 20/1 as eluent to give the product with a yield of 80 %. ^{1}H NMR (300 MHz, DMSO-d_6, δ) 10.12 (s, 2H), 7.41–7.33 (m, 10H), 7.16–7.10 (m, 6H), 6.95–6.90 (m, 2H), 6.89–6.82 (m, 4H). ^{13}C NMR (75 MHz, DMSO-d_6) δ: 160.5, 150.2, 146.2, 133.5, 133.4, 132.8, 132.7, 129.9, 125.7, 124.6, 123.4, 122.3, 119.6, 119.5, 115.6, 115.5. ^{31}P NMR (DMSO-d_6, 295 K, δ): 25.58. MALDI-TOF MS: calcd for $C_{30}H_{24}NO_3P$: 477.1. found: 478.1 $[M + H]^+$. Anal. calcd for $C_{30}H_{24}NO_3P$: C, 75.46; H, 5.07; N, 2.93; found: C, 75.27; H, 5.00; N, 2.88.

Br-Cz-MON. This compound was prepared from **3** and **8** according to the procedure for the synthesis of F-Cz-MON. Column chromatography on silica gel using petroleum ether/ethyl acetate = 2/1 as eluent gave the crude product, which was crystallized in a mixture of petroleum ether and CH_2Cl_2 to give the pure product as white crystal in an overall yield of 78 %. ^{1}H NMR (300 MHz, $CDCl_3$) δ 8.13 (d, J = 1.8 Hz, 2H), 7.83 (dd, J = 11.5, 8.3 Hz, 2H), 7.74–7.67 (m, 6H), 7.62 (dd, J = 11.2, 8.5 Hz, 4H), 7.46 (dd, J = 8.7, 1.8 Hz 2H), 7.42 (d, J = 8.7 Hz, 2H), 1.46 (s, 18H). ^{13}C NMR (75 MHz, $CDCl_3$) δ: 143.8, 142.3, 138.4, 133.6, 132.2, 132.1, 131.5, 130.5, 127.7, 126.2, 126.1, 123.9, 116.4, 109.1, 34.7, 31.9. ^{31}P NMR ($CDCl_3$, 295 K, δ): 27.14. MALDI-TOF MS: calcd for $C_{38}H_{36}Br_2NOP$: 713.1. found: 714.1 $[M + H]^+$. Anal. calcd for $C_{38}H_{36}Br_2NOP$: C, 63.97; H, 5.09; N, 1.96; found: C, 63.79; H, 4.98; N, 1.90.

Br-DPA-MON. This compound was prepared from **3** and **7** according to the procedure for the synthesis of F-Cz-MON. Column chromatography on silica gel

using petroleum ether/ethyl acetate = 3/2 as eluent gave the product in 65 % yield. ^{1}H NMR (300 MHz, $CDCl_3$) δ7.61 (dd, J = 11.1, 2.7 Hz, 4H) 7.54 (dd, J = 11.4, 8.4 Hz, 4H), 7.37 (dd, J = 11.7, 8.7 Hz, 2H), 7.33–7.28 (m, 4H), 7.15–7.10 (m, 6H), 7.01 (dd, J = 8.8, 2.4 Hz, 2H). ^{13}C NMR (75 MHz, $CDCl_3$) 151.5, 146.3, 133.5, 133.4, 132.2, 131.9, 131.8, 131.2, 129.6, 127.2, 125.9, 124.7, 119.9, 119.8. δ: ^{31}P NMR ($CDCl_3$, 295 K, δ): 27.51. MALDI-TOF MS: calcd for $C_{30}H_{22}Br_2NOP$: 601.0. found: 602.0 $[M + H]^+$. Anal. calcd for $C_{30}H_{22}Br_2NOP$: C, 59.73; H, 3.68; N, 2.32; found: C, 59.60; H, 3.58; N, 2.22.

MC. This compound was prepared from **1** and **6** according to the procedure for the synthesis of F-Cz-MON. Column chromatography on silica gel using petroleum ether/ethyl acetate = 2/1 as eluent gave the product in 90 % yield. ^{1}H NMR (300 MHz, $CDCl_3$, δ): 8.13 (d, J = 1.6 Hz, 2H), 7.85 (dd, J = 11.5, 8.5 Hz, 2H), 7.71–7.64 (m, 6H), 7.47 (dd, J = 8.7, 1.8 Hz, 2H), 7.42 (d, J = 8.6 Hz, 2H), 7.03 (dd, J = 8.8, 2.2 Hz, 4H), 3.88 (s, 6H), 1.46 (s, 18H). ^{13}C NMR (75 MHz, $CDCl_3$, δ): 162.5, 143.5, 141.5, 138.6, 134.0, 133.6, 125.9, 124.4, 123.8, 123.3, 116.3, 114.2, 109.2, 55.4, 34.7, 31.2. ^{31}P NMR ($CDCl_3$, 295 K, δ): 28.11. MALDI-TOF MS: calcd for $C_{40}H_{42}NO_3P$: 615.3. found: 616.2 $[M + H]^+$. Anal. calcd for $C_{40}H_{42}NO_3P$: C, 78.02; H, 6.88; N, 2.27. found: C, 77.90; H, 6.79; N, 2.20.

PCzPO. Under argon, F-Cz-MON (0.2959 g, 0.5 mmol), HO-Cz-MON (0.2351 g, 0.5 mmol), K_2CO_3 (0.21 g, 1.5 mmol), *N*, *N*-dimethylacetamide (2.0 mL) and toluene (3.0 mL) were added to a 10 mL flask equipped with a magnetic stir bar, oil-water separator, and gas adapter. The reaction was stirred at 140 °C for 3 h and then 165 °C for 24 h. After cooling to room temperature, the mixture was extracted with CH_2Cl_2. The organic phase was washed with water and then dried over Na_2SO_4. The solution was concentrated and then precipitated in methanol to afford PCzPO as white fiber (0.42 g) in 74 % yield. ^{1}H NMR (400 MHz, $CDCl_3$, δ): 8.12 (s, 2H), 7.91–7.86 (m, 2H), 7.81–7.71 (m, 6H), 7.45–7.40 (m, 4H), 7.20 (d, J = 7.5 Hz, 4H), 1.44 (s, 18H). ^{31}P NMR ($CDCl_3$, 295 K, δ): 27.20. Anal. Calcd for $(C_{38}H_{36}NO_2P)_n$: C, 80.12; H, 6.37; N, 2.46. found: C, 79.96; H, 6.29; N, 2.40.

PDPAPO. This polymer was prepared from F-DPA-MON (0.1926 g, 0.40 mmol) and HO-DPA-MON (0.1910 g, 0.40 mmol) according to the procedure for the synthesis of PCzPO in 55 % yield. ^{1}H NMR (300 MHz, $CDCl_3$, δ): 7.71–7.65 (m, 4H), 7.44–7.38 (m, 2H), 7.31–7.24 (m, 4H), 7.14–7.06 (m, 10H), 7.01 (d, J = 7.2 Hz, 2H). ^{31}P NMR ($CDCl_3$, 295 K, δ):.27.66, Anal. Calcd for $(C_{30}H_{22}NO_2P)_n$: C, 78.42; H, 4.83; N, 3.05; found: C, 78.21; H, 4.73; N, 2.98.

PCzP. To a mixture of $Ni(COD)_2$ (0.55 g, 2 mmol) and 2,2′-bipyridyl (0.31 g, 2 mmol), 0.25 mL 1,5-cyclooctadiene (COD) and 3 mL anhydrous DMF were added under argon. The resulting mixture was kept stirring at 80 °C for 0.5 h. Then a solution of Br-Cz-MON (0.7135 g, 1 mmol) in 3 mL DMF was slowly added to the mixture. The reaction was maintained at 80 °C for 24 h in dark. After cooling to room temperature, the obtained mixture was poured to DCM, then washed intensively with saturated ethylenediaminetetraacetic acid tetrasodium aqueous solution and distilled water. After dried with anhydrous sodium sulfate, the organic phase was concentrated to an appropriate volume and then precipitated in methanol to get

a white fiber (0.28 g, yield 50 %). ^{1}H NMR (300 MHz, $CDCl_3$) δ 8.12 (br, 2H), 7.96–7.89 (m, 6H), 7.82–7.73 (m, 6H), 7.47–7.43 (m, 4H), 1.45 (br, 18H). ^{31}P NMR ($CDCl_3$, 295 K, δ): 27.58. Anal. Calcd for $(C_{38}H_{36}NOP)_n$: C, 82.43; H, 6.55; N, 2.53; found: C, 82.31; H, 6.50; N, 2.43.

PDPAP. This polymer was prepared from Br-DPA-MON (0.8000 g, 1.33 mmol) according to the procedure for PCzP in 31 % yield. ^{1}H NMR (300 MHz, $CDCl_3$) δ 7.80 (dd, J = 10.2, 8.4 Hz, 1H), 7.67 (d, J = 6.9 Hz, 4H), 7.44 (dd, J = 10.8, 9.0 Hz, 2H), 7.31–7.27 (m, 4H), 7.13–7.06 (m, 6H), 7.01 (d, J = 7.3 Hz, 2H). ^{31}P NMR ($CDCl_3$, 295 K, δ): 28.04. Anal. Calcd for $(C_{30}H_{22}NOP)_n$: C, 81.25; H, 5.00; N, 3.16; found: C, 81.07; H, 4.92; N, 3.06.

References

1. Baldo MA, O'Brien DF, You Y et al (1998) Highly efficient phosphorescent emission from organic electroluminescent devices. Nature 395:151–154
2. Kawamura Y, Yanagida S, Forrest SR (2002) Energy transfer in polymer electrophosphorescent light emitting devices with single and multiple doped luminescent layers. J Appl Phys 92:87–93
3. Gong X, Ma WL, Ostrowski JC et al (2004) White electrophosphorescence from semiconducting polymer blends. Adv Mater 16:615–619
4. Sudhakar M, Djurovich PI, Hogen-Esch TE et al (2003) Phosphorescence quenching by conjugated polymers. J Am Chem Soc 125:7796–7797
5. Chou HH, Cheng CH (2010) A highly efficient universal bipolar host for blue, green, and red phosphorescent OLEDs. Adv Mater 22:2468–2471
6. Polikarpov E, Swensen JS, Chopra N et al (2009) An ambipolar phosphine oxide-based host for high power efficiency blue phosphorescent organic light emitting devices. Appl Phys Lett 94:223304
7. Jeon SO, Yook KS, Joo CW et al (2010) High-efficiency deep-blue-phosphorescent organic light-emitting diodes using a phosphine oxide and a phosphine sulfide high-triplet-energy host material with bipolar charge-transport properties. Adv Mater 22:1872–1876
8. van Dijken A, Bastiaansen J, Kiggen NMM et al (2004) Carbazole compounds as host materials for triplet emitters in organic light-emitting diodes: polymer hosts for high-efficiency light-emitting diodes. J Am Chem Soc 126:7718–7727
9. Brunner K, van Dijken A, Borner H et al (2004) Carbazole compounds as host materials for triplet emitters in organic light-emitting diodes: tuning the HOMO level without influencing the triplet energy in small molecules. J Am Chem Soc 126:6035–6042
10. Chen YC, Huang GS, Hsiao CC et al (2006) High triplet energy polymer as host for electrophosphorescence with high efficiency. J Am Chem Soc 128:8549–8558
11. Zhang K, Tao Y, Yang C et al (2008) Synthesis and properties of carbazole main chain copolymers with oxadiazole pendant toward bipolar polymer host: tuning the HOMO/LUMO level and triplet energy. Chem Mater 20:7324–7331
12. Mathai MK, Choong V-E, Choulis SA et al (2006) Highly efficient solution processed blue organic electrophosphorescence with 14 Lm/W luminous efficacy. Appl Phys Lett 88:243512
13. Shao S, Ding J, Ye T et al (2011) A novel, bipolar polymeric host for highly efficient blue electrophosphorescence: a non-conjugated poly(aryl ether) containing triphenylphosphine oxide units in the electron-transporting main chain and carbazole units in hole-transporting side chains. Adv Mater 23:3570–3574
14. Nielsen KT, Bechgaard K, Krebs FC (2005) Removal of palladium nanoparticles from polymer materials. Macromolecules 38:658–659

15. Sapochak LS, Padmaperuma AB, Cai XY et al (2008) Inductive effects of diphenylphosphoryl moieties on carbazole host materials: design rules for blue electrophosphorescent organic light-emitting devices. J Phys Chem C 112:7989–7996
16. Ding J, Wang Q, Zhao L et al (2010) Design of star-shaped molecular architectures based on carbazole and phosphine oxide moieties: towards amorphous bipolar hosts with high triplet energy for efficient blue electrophosphorescent devices. J Mater Chem 20:8126–8133
17. Yeh HC, Chien CH, Shih PI et al (2008) Polymers derived from 3,6-fluorene and tetraphenylsilane derivatives: solution-processable host materials for green phosphorescent OLEDs. Macromolecules 41:3801–3807

http://www.springer.com/978-3-662-44375-0

Electrophosphorescent Polymers Based on Polyarylether Hosts

Shao, S.

2014, XIII, 96 p. 71 illus., 22 illus. in color., Hardcover
ISBN: 978-3-662-44375-0